# Magnetic dipole transitions in superdeformed nuclei

K. Sugawara-Tanabe,[1,2] A. Arima,[2] and N. Yoshida[2,3]
[1]*Otsuma Women's University, Tama, Tokyo 206, Japan*
[2]*The Institute of Physical and Chemical Research, Wako, Saitama 351-01, Japan*
[3]*Faculty of Informatics, Kansai University, Takatsuki, Osaka 569, Japan*
(Received 7 August 1995)

Magnetic dipole transition matrix elements in superdeformed nuclei are calculated based on an axially symmetrically deformed Nilsson model. Several levels become the candidates to be assigned for the experimental evidence of the superdeformed band in $^{193}$Hg and $^{193}$Tl. Although the intrinsic $g_K$ factors for some levels show slower convergence to the asymptotic limit values, their wave functions show a good revival of $L-S$ coupling scheme at superdeformation. Comparing the experimental data with the renormalized $g_K'$, we find the pseudospin picture is not suitable for the superdeformed band.

PACS number(s): 21.10.Ky, 21.10.Pc, 21.60.Cs, 27.80.+w

## I. INTRODUCTION

We have shown that the $L-S$ coupling scheme is restored for the superdeformed (SD) states, and proposed the idea that the quantization of alignment at SD bands is related with the real spin [1,2] and not with the pseudospin mechanism which is a good approximation for a usual deformed nuclei [3,4]. In order to confirm our conclusion in the previous paper [2], we calculate $M1$ matrix elements, as the magnetic properties can provide insights into the single-particle structure and clarify the difference between the pseudo $\tilde{L}\cdot\tilde{S}$ and the real $L\cdot S$ coupling schemes. Recently experimental evidence for $M1$ transitions in $^{193}$Hg [5] and $^{193}$Tl [6] were reported, where the $M1$ matrix elements are extracted. The theoretical analysis based on the particle-rotor model is published and supports the assigment of the odd neutron in the [512]5/2 orbital in the $^{193}$Hg case [7].

In this paper we make a survey of theoretical $g_K$ values for one single-particle SD rotational band in $^{193}$Hg, $^{193}$Tl, and also $^{153}$Dy and $^{153}$Ho in which no experimental data are reported yet. The calculation is performed using a Nicra code [8] with the same parameter set as in the previous paper [2]. The purpose of this investigation is to identify additional configurations that are expected to lie close to the Fermi surface with observable $M1$ strength, and to discuss their intrinsic structure in connection with the $L-S$ coupling scheme. We found that the values of $g_K$ for some levels do not yet reach to the asymptotic values although their wave functions show enough revival of the $L-S$ coupling scheme. This is because of the cancellation between two kinds of summed squared amplitudes with $\Omega=J_z=L_z+S_z=\Lambda\pm 1/2$. For the case of the proton shell, there is another cancellation between the orbital term and the spin term of the $M1$ operator in addition to this cancellation. However their wave func-

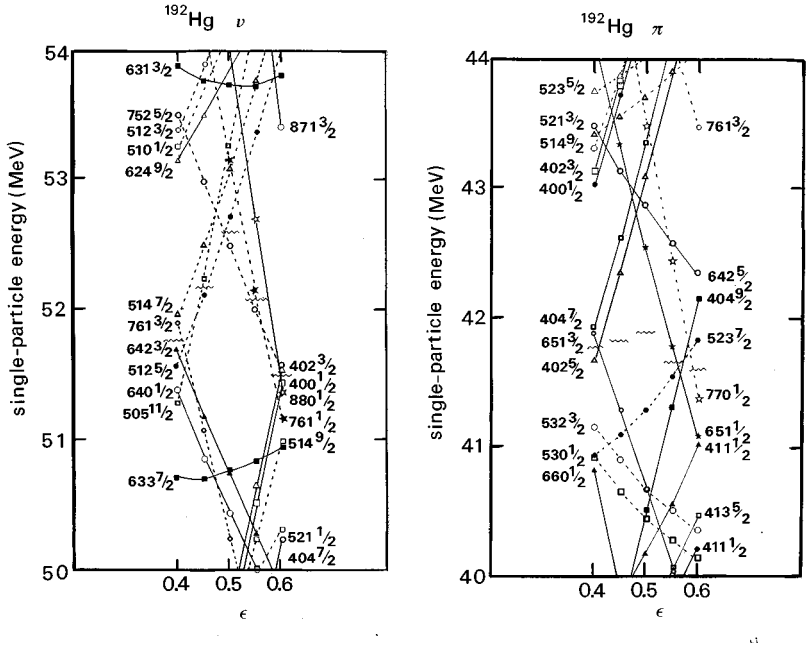


FIG. 1. The calculated energies $E(\sigma,\Omega)$ as a function of the ellipsoidal deformation $\epsilon$ for the neutron shell ($\nu$) and the proton shell ($\pi$) in $^{192}$Hg. The ordinate is in units of MeV. All $E(\sigma,\Omega)$ are obtained by diagonalizing the total $H$, but labeled by asymptotic quantum numbers $Nn_z\Lambda\Omega$, to which they converge at very large deformation. The positive-parity levels are shown by solid lines, while the negative-parity levels by dashed lines. The Fermi surfaces are denoted by wavy lines. The values of $\epsilon$ are from 0.4 to 0.6.

 

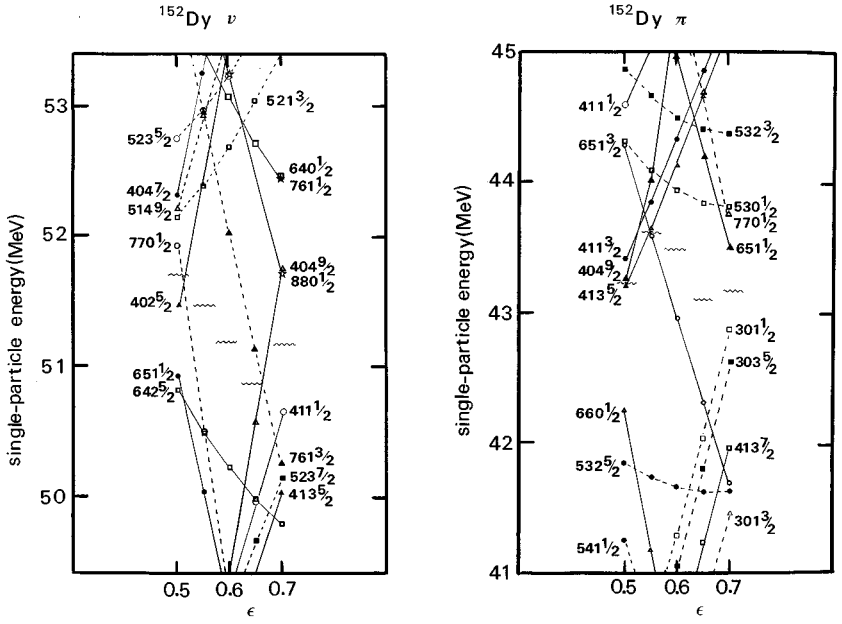


FIG. 2. The same quantities as in Fig.1 for $^{152}$Dy. The values of $\epsilon$ are from 0.5 to 0.7.

tions show a quite good revival of the $L-S$ coupling scheme. We compared the renormalized $g_K'$ based on the pseudospin picture and the original $g_K$ based on the real spin picture, and found that the pseudospin mechanism is not a good approximation for the superdeformed band.

## II. $g_K$ VALUES

In the strong coupling limit the $B(M1)$ values for a $K$ band can be written

$$B(M1;I_iK\rightarrow I_fK)=\frac{3}{4\pi}(g_K-g_R)^2K^2\mu_N^2, \qquad (1)$$

where $g_R$ is the rotational $g$ factor and the intrinsic $g$ factor $g_K$ is defined by

$$g_K\Omega=g_\ell\langle\sigma,\Omega|\ell_z|\sigma,\Omega\rangle+g_s\langle\sigma,\Omega|s_z|\sigma,\Omega\rangle. \qquad (2)$$

Throughout the paper we shall use $g_\ell=g_\ell^{\rm free}$ and $g_s=0.8g_s^{\rm free}$, which are used in [5]. In (2) the wave function is the eigenvector of the Hamiltonian $H$ given by

$$H|\sigma,\Omega\rangle=E(\sigma,\Omega)|\sigma,\Omega\rangle, \qquad (3)$$

where $\Omega=J_z$ and $\sigma$ represents all the other quantum numbers.

We show single-particle energies $E(\sigma,\Omega)$ as a function of the deformation $\epsilon$, which is equal to $\delta_{\rm osc}$ adopted in a previous paper [1,2], in Fig. 1 (Hg case) and in Fig. 2 (Dy case) both for the neutron shell ($\nu$) and for the proton shell ($\pi$). The single-particle levels are labeled by the asymptotic quantum numbers $[Nn_z\Lambda]\Omega$, and the Fermi surface of the nucleus at each deformation is shown by a wavy line inside the figures. We calculated $g_K$ values for those levels lying close to the Fermi surface shown in Figs. 1 and 2. In Fig. 3 the calculated $g_k$ values for the neutron levels of $^{192}$Hg lying near to the Fermi surface are shown as a function of $\epsilon$. As is shown in the figure, $g_K$ with a small value of $\Omega$ depends on the deformation $\epsilon$ more strongly than those with large $\Omega$. It is partly because the division by small $\Omega$ in (2) enhances the change of $\mu_z$. Another reason is that the single-particle level with small $\Omega$ in large $N$ depends on the deformation more strongly than that with large $\Omega$ as is seen in $E(\sigma,\Omega)$. Comparing with the experimental values of $g_K=-0.65\pm0.14$ and $\Omega=2.8\pm0.8$, [5] only the [512]5/2 level is the candidate around $\epsilon\sim0.5$. However if the experimental assignment of $\Omega$ is not taken seriously, [631]3/2, [761]3/2, [871]3/2, and [761]1/2 also become the candidates to explain the experimental $g_K$ value. Here we assume that single-particle levels of $^{192}$Hg are nearly the same as those of $^{193}$Hg.

If the $L-S$ coupling is completely resurrected, the value

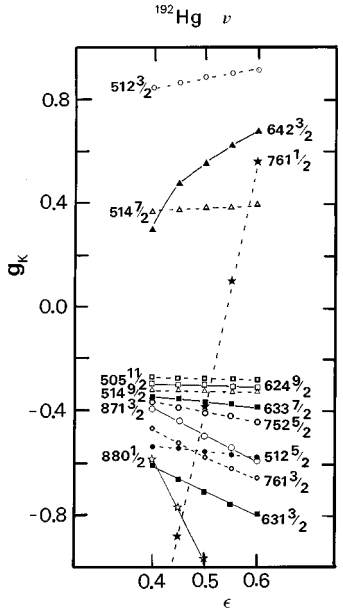


FIG. 3. The values of $g_K$ as a function of $\epsilon$ for the neutron shell ($\nu$) in $^{192}$Hg. The symbols are the same as given in Fig. 1. The positive-parity levels are shown by solid lines, and the negative-parity levels by dashed lines. The values of $\epsilon$ are from 0.4 to 0.6.

TABLE I. The values of $g_K$ and $\langle\sigma,\Omega|s_z|\sigma,\Omega\rangle$ (inside the parentheses) as a function of deformation $\epsilon$ for single-particle levels in $^{192}$Hg. The values in the fifth and tenth columns denote the limiting values of $g_K$ evaluated by the asymptotic wave function.

| | Neutron | | | | | Proton | | | |
|---|---|---|---|---|---|---|---|---|---|
| Level\$\epsilon$ | 0.4 | 0.5 | 0.6 | Limit | Level\$\epsilon$ | 0.4 | 0.5 | 0.6 | Limit |
| $400\frac{1}{2}$ | -2.91 | -2.95 | -2.98 | -3.06 | $411\frac{1}{2}$ | -1.88 | -2.04 | -2.14 | -2.46 |
| | (0.475) | (0.482) | (0.486) | | | (-0.416) | (-0.439) | (-0.454) | |
| $402\frac{3}{2}$ | 0.959 | 0.974 | 0.985 | 1.02 | $413\frac{5}{2}$ | 0.422 | 0.394 | 0.374 | 0.308 |
| | (-0.470) | (-0.478) | (-0.483) | | | (-0.418) | (-0.438) | (-0.452) | |
| $512\frac{5}{2}$ | -0.532 | -0.553 | -0.567 | -0.612 | $402\frac{5}{2}$ | 1.67 | 1.68 | 1.68 | 1.69 |
| | (0.435) | (0.452) | (0.463) | | | (0.485) | (0.489) | (0.492) | |
| $514\frac{7}{2}$ | 0.367 | 0.383 | 0.394 | 0.437 | $404\frac{7}{2}$ | 0.537 | 0.530 | 0.525 | 0.506 |
| | (-0.42) | (-0.438) | (-0.451) | | | (-0.469) | (-0.475) | (-0.480) | |
| $514\frac{9}{2}$ | -0.319 | -0.323 | -0.326 | -0.340 | $530\frac{1}{2}$ | 2.94 | 3.39 | 3.69 | 4.46 |
| | (0.469) | (0.475) | (0.480) | | | (0.280) | (0.345) | (0.389) | |
| $640\frac{1}{2}$ | -1.16 | -1.70 | -2.07 | -3.06 | $532\frac{3}{2}$ | 0.363 | 0.222 | 0.123 | -0.153 |
| | (0.189) | (0.277) | (0.338) | | | (-0.276) | (-0.338) | (-0.380) | |
| $642\frac{3}{2}$ | 0.392 | 0.555 | 0.674 | 1.02 | $521\frac{3}{2}$ | 1.85 | 1.94 | 1.99 | 2.15 |
| | (-0.192) | (-0.272) | (-0.331) | | | (0.369) | (0.405) | (0.429) | |
| $631\frac{3}{2}$ | -0.608 | -0.719 | -0.795 | -1.02 | $523\frac{7}{2}$ | 1.43 | 1.44 | 1.45 | 1.49 |
| | (0.298) | (0.352) | (0.390) | | | (0.435) | (0.448) | (0.459) | |
| $633\frac{7}{2}$ | -0.349 | -0.366 | -0.380 | -0.437 | $651\frac{1}{2}$ | 0.786 | -0.145 | -0.859 | -2.46 |
| | (0.399) | (0.419) | (0.435) | | | (-0.031) | (-0.165) | (-0.269) | |
| $761\frac{1}{2}$ | -1.32 | -0.377 | 0.551 | 3.06 | $651\frac{3}{2}$ | 1.68 | 1.79 | 1.88 | 2.15 |
| | (0.216) | (0.06) | (-0.09) | | | (0.294) | (0.343) | (0.381) | |
| $761\frac{3}{2}$ | -0.472 | -0.571 | -0.695 | -1.02 | $642\frac{5}{2}$ | 1.49 | 1.53 | 1.57 | 1.69 |
| | (0.232) | (0.280) | (0.323) | | | (0.353) | (0.384) | (0.409) | |
| $752\frac{5}{2}$ | -0.362 | -0.404 | -0.440 | -0.612 | $770\frac{1}{2}$ | 1.95 | 2.45 | 2.95 | 4.46 |
| | (0.296) | (0.330) | (0.359) | | | (0.137) | (0.210) | (0.282) | |
| $880\frac{1}{2}$ | -0.591 | -0.968 | -1.42 | -3.06 | $761\frac{3}{2}$ | 1.53 | 1.65 | 1.75 | 2.15 |
| | (0.097) | (0.158) | (0.232) | | | (0.232) | (0.280) | (0.323) | |
| $871\frac{3}{2}$ | -0.394 | -0.490 | -0.585 | -1.02 | | | | | |
| | (0.193) | (0.240) | (0.287) | | | | | | |

of $\langle\sigma,\Omega|s_z|\sigma,\Omega\rangle$ becomes $\pm 1/2$ corresponding to $\Omega=\Lambda\pm 1/2$. Then the $g_K$ for the neutron (proton) single-particle level, $g_K(\nu)[g_K(\pi)]$ becomes

$$g_K(\nu)=\pm g_s^{\nu}\frac{1}{2\Omega},\quad g_K(\pi)=1\pm(g_s^{\pi}-1)\frac{1}{2\Omega}. \qquad (4)$$

The $\pm$ sign corresponds to $\Omega=\Lambda\pm 1/2$, respectively. In Table I we show $g_K$ values according with an increasing $\epsilon$ together with the asymptotic values calculated from (4). Comparing values in the fourth column with those in the fifth column in Table I, we find most of the levels show a good convergence to the asymptotic values. But $g_K$ of the [761]1/2, [880]1/2, and [871]3/2 levels in the $\nu$ shell do not yet approach 60% of the limit value at $\epsilon=0.6$, although they show a good tendency. In the same table we showed $\langle\sigma,\Omega|s_z|\sigma,\Omega\rangle$ inside the parentheses just below the $g_k$ value corresponding to each level and deformation. They show a good tendency to reach $\pm 1/2$ with increasing $\epsilon$. The absolute values of $\langle\sigma,\Omega|s_z|\sigma,\Omega\rangle$ for the [761]1/2, [880]1/2, and [871]3/2 levels are smaller than $|0.3|$ at $\epsilon=0.6$. At $\epsilon=0.8$, $\langle\sigma,\Omega|s_z|\sigma,\Omega\rangle$ for the [761]1/2, [880]1/2, and [871]3/2 levels become $-0.29$, $-0.35$, and 0.36, and their $g_K$ values are 1.78, $-2.17$, and $-0.74$, respectively. Thus their ratios to the limit values become much better, i.e., 59%, 71%, and 73%.

In a previous paper [2] we proved the resurrection of $L-S$ coupling in the follwing way. The eigenstate of (3) is expanded by $L-S$ coupled spherical basis $|N,L,L_z=\Lambda,\Omega\rangle$ utilizing the formula

$$|\sigma,\Omega\rangle=\sum_{L,\Lambda} W^{\sigma,\Omega}_{N,L,\Lambda,\Omega}|N,L,\Lambda,\Omega), \qquad (5)$$

where the sum over $\Lambda$ runs over only two terms, i.e., $\Omega+1/2$ and $\Omega-1/2$. Then we compared two summed squares of amplitudes over $L$, i.e., $\Sigma_L|W^{\sigma,\Omega}_{N,L,\Lambda,\Omega}|^2$ for fixed $\Lambda=\Omega\pm 1/2$, respectively. In Table II we show these two sums within the interval of $0.0\leqslant\epsilon\leqslant 0.8$. For example, in the case of [871]3/2, the amplitude with $\Lambda=1$ to that with $\Lambda=2$ is 0.588 to 0.412 at $\epsilon=0.0$, and 0.864 to 0.136 at $\epsilon=0.8$. We find quite good revival of the $L-S$ coupling scheme even for those levels whose $g_K$ do not show enough convergence to the asymptotic values.

TABLE II. The summed values of $\Sigma_L|W^{\sigma,\Omega}_{N,L,\Omega-\frac{1}{2},\Omega}|^2$ (upper row) and $\Sigma_L|W^{\sigma,\Omega}_{N,L,\Omega+\frac{1}{2},\Omega}|^2$ (lower row) as a function of deformation ($\epsilon$) for the single-particle level in $^{192}$Hg.

| | | Neutron | | | | | | |
|---|---|---|---|---|---|---|---|---|
| $\epsilon$ | Level | $640\frac{1}{2}$ | $642\frac{3}{2}$ | $631\frac{3}{2}$ | $761\frac{1}{2}$ | $761\frac{3}{2}$ | $880\frac{1}{2}$ | $871\frac{3}{2}$ |
| 0.0 | | 0.461 | 0.666 | 0.385 | 0.546 | 0.601 | 0.530 | 0.588 |
| | | 0.539 | 0.334 | 0.615 | 0.454 | 0.399 | 0.470 | 0.412 |
| 0.2 | | 0.571 | 0.547 | 0.586 | 0.663 | 0.643 | 0.541 | 0.621 |
| | | 0.429 | 0.453 | 0.414 | 0.337 | 0.357 | 0.459 | 0.379 |
| 0.4 | | 0.689 | 0.308 | 0.798 | 0.716 | 0.731 | 0.596 | 0.692 |
| | | 0.311 | 0.692 | 0.202 | 0.284 | 0.269 | 0.404 | 0.308 |
| 0.6 | | 0.838 | 0.169 | 0.889 | 0.409 | 0.823 | 0.731 | 0.787 |
| | | 0.162 | 0.831 | 0.111 | 0.591 | 0.177 | 0.269 | 0.213 |
| 0.8 | | 0.912 | 0.095 | 0.935 | 0.209 | 0.890 | 0.855 | 0.864 |
| | | 0.088 | 0.905 | 0.065 | 0.791 | 0.110 | 0.145 | 0.136 |
| | | Proton | | | | | | |
| $\epsilon$ | Level | $532\frac{3}{2}$ | $521\frac{3}{2}$ | $523\frac{7}{2}$ | $651\frac{1}{2}$ | $651\frac{3}{2}$ | $642\frac{5}{2}$ | $770\frac{1}{2}$ |
| 0.0 | | 0.714 | 0.364 | 0.819 | 0.555 | 0.615 | 0.692 | 0.533 |
| | | 0.286 | 0.636 | 0.181 | 0.445 | 0.385 | 0.308 | 0.467 |
| 0.2 | | 0.436 | 0.713 | 0.892 | 0.703 | 0.684 | 0.772 | 0.552 |
| | | 0.564 | 0.287 | 0.108 | 0.297 | 0.316 | 0.228 | 0.448 |
| 0.4 | | 0.223 | 0.868 | 0.935 | 0.469 | 0.794 | 0.854 | 0.636 |
| | | 0.777 | 0.132 | 0.065 | 0.531 | 0.206 | 0.146 | 0.364 |
| 0.6 | | 0.120 | 0.929 | 0.959 | 0.232 | 0.881 | 0.910 | 0.782 |
| | | 0.880 | 0.071 | 0.041 | 0.768 | 0.119 | 0.090 | 0.218 |
| 0.8 | | 0.067 | 0.959 | 0.974 | 0.112 | 0.932 | 0.942 | 0.886 |
| | | 0.933 | 0.041 | 0.026 | 0.888 | 0.068 | 0.058 | 0.114 |

This discrepancy is explained in the following way. With the help of (5), the expectation value of $\langle\sigma,\Omega|s_z|\sigma,\Omega\rangle>$ is given by

$$\langle\sigma,\Omega|s_z|\sigma,\Omega\rangle=\frac{1}{2}\sum_L\ (|W^{\sigma,\Omega}_{N,L,\Omega-\frac{1}{2},\Omega}|^2-|W^{\sigma,\Omega}_{N,L,\Omega+\frac{1}{2},\Omega}|^2). \tag{6}$$

Thus even when the $L-S$ scheme becomes pretty good, $\langle\sigma,\Omega|s_z|\sigma,\Omega\rangle$ is calculated by the subtraction between two components. The ratio of the $g_K$ value at a fixed $\epsilon$ to the asymptotic limit value is given by the ratio of the expectation value of $s_z$ to $\pm1/2$. As $\Sigma_L|W^{\sigma,\Omega}_{N,L,\Omega-\frac{1}{2},\Omega}|^2+\Sigma_L|W^{\sigma,\Omega}_{N,L,\Omega+\frac{1}{2},\Omega}|^2=1$, the ratio becomes the difference between two components at the same $\epsilon$. For example, in the [631]3/2 level of the $\nu$ shell at the $\epsilon=0.6$ case, the ratio of $g_K$ to the asymptotic value, i.e., 0.795/1.02 (see Table I) is the same as the difference between the $\Lambda=1$ and $\Lambda=2$ components, i.e., $0.889-0.111$ (see Table II). Subtraction between the two components smears the convergence to the limit. This is the reason why $g_K$ does not converge enough to the asymptotic value even when the squared amplitude of the component with the same $\Lambda$ as the asymptotic quantum number $\Lambda_{aq}$ shows a quite good convergence.

We showed the values of $g_K$ and $\langle\sigma,\Omega|s_z|\sigma,\Omega\rangle$ for the proton shell in $^{192}$Hg in the right column of Table I. Similarly we see not enough convergence to the asymptotic limit for [532]3/2 and [651]1/2, although the expectation value of $s_z$ for [532]3/2 is quite good (larger than $|0.3|$) compared with the other levels. The summed squares of two amplitudes for proton levels are also shown in the lower half raw of Table II. At $\epsilon=0.8$ the difference between two amplitudes is 0.86 for [532]3/2 and 0.76 for [651]1/2, and $\langle\sigma,\Omega|s_z(\pi)|\sigma,\Omega\rangle$ is $-0.46$ for [532]3/2, $-0.39$ for [651]1/2. However $g_K$ is 0.0019 for [532]3/2 and $-1.00$ for [651]1/2 even at $\epsilon=0.8$. The proton case is not so simple compared with the neutron case, as $g_K(\pi)$ depends not only on $\langle\sigma,\Omega|s_z(\pi)|\sigma,\Omega\rangle$ but also on $\langle\sigma,\Omega|l_z(\pi)|\sigma,\Omega\rangle$. Moreover even when $\langle\sigma,\Omega|s_z|\sigma,\Omega\rangle$ becomes nearly $\pm1/2$, as is the case for [532]3/2, the large factor $g_s(\pi)$ enhances the small difference. When $\langle\sigma,\Omega|s_z(\pi)|\sigma,\Omega\rangle$ is negative, the cancellation between $s_z$ and $l_z$ in (2) prohibits $g_K$ to converge to the limit. This is the case for [532]3/2 and [651]1/2.

The experimental evidence for $M1$ transitions in the superdeformed bands of $^{193}$Tl is recently reported [6]. It gives $(g_K-g_R)K/Q_0=0.12$–$0.15$ for the superdeformed band. We assume the same value of $Q_0$ as adopted in $^{193}$Hg [5], $g_R=Z/A$ and the same proton single-particle levels for $^{193}$Tl as those for $^{192}$Hg. Then $g_K$ estimated from this experimental data becomes 6.11–4.97 for $K=1/2$, 2.31–1.93 for $K=3/2$, and 1.55–1.32 for $K=5/2$. As is seen in the right

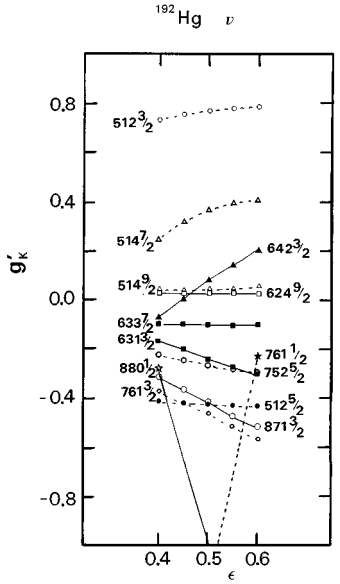


FIG. 4. The renormalized values of $g_K$ factor, $g'_K$ (dropping the contribution from the unique-parity level) as a function of $\epsilon$ for the neutron shell ($\nu$) in $^{192}$Hg. The symbols are the same as given in Fig. 3. The positive-parity levels are shown by solid lines, and the negative-parity levels by dashed lines. The values of $\epsilon$ are from 0.4 to 0.6.

TABLE III. The values of $g_K$ and $\langle\sigma,\Omega|s_z|\sigma,\Omega\rangle$ (inside the parentheses) as a function of deformation $\epsilon$ for single-particle levels in $^{152}$Dy. The values in the fifth and tenth columns denote the limiting values of $g_K$ evaluated by the asymptotic wave function.

| | Neutron | | | | | Proton | | | |
|---|---|---|---|---|---|---|---|---|---|
| Level\$\epsilon$ | 0.5 | 0.6 | 0.7 | Limit | Level\$\epsilon$ | 0.5 | 0.6 | 0.7 | Limit |
| $411\frac{1}{2}$ | 2.43 | 2.58 | 2.69 | 3.06 | $301\frac{1}{2}$ | -2.12 | -2.19 | -2.25 | -2.46 |
| | (-0.398) | (-0.421) | (-0.439) | | | (-0.451) | (-0.462) | (-0.470) | |
| $402\frac{5}{2}$ | -0.583 | -0.591 | -0.600 | -0.612 | $303\frac{5}{2}$ | 0.370 | 0.359 | 0.350 | 0.308 |
| | (0.476) | (0.483) | (0.487) | | | (-0.455) | (-0.463) | (-0.469) | |
| $521\frac{3}{2}$ | -0.749 | -0.816 | -0.863 | -1.02 | $411\frac{3}{2}$ | 2.02 | 2.05 | 2.07 | 2.15 |
| | (0.367) | (0.400) | (0.423) | | | (0.444) | (0.455) | (0.464) | |
| $523\frac{7}{2}$ | -0.381 | -0.391 | -0.399 | -0.437 | $413\frac{5}{2}$ | 0.419 | 0.397 | 0.380 | 0.308 |
| | (0.436) | (0.447) | (0.457) | | | (-0.420) | (-0.436) | (-0.448) | |
| $514\frac{9}{2}$ | -0.319 | -0.323 | -0.326 | -0.340 | $413\frac{7}{2}$ | 1.46 | 1.46 | 1.47 | 1.49 |
| | (0.470) | (0.475) | (0.479) | | | (0.468) | (0.474) | (0.478) | |
| $640\frac{1}{2}$ | 1.00 | -1.47 | -2.00 | -3.06 | $530\frac{1}{2}$ | 2.82 | 3.28 | 3.60 | 4.46 |
| | (0.164) | (0.256) | (0.321) | | | (0.263) | (0.330) | (0.375) | |
| $642\frac{5}{2}$ | -0.446 | -0.477 | -0.503 | -0.612 | $532\frac{3}{2}$ | -0.387 | -0.242 | -0.143 | -0.153 |
| | (0.365) | (0.390) | (0.411) | | | (-0.266) | (-0.328) | (-0.372) | |
| $770\frac{1}{2}$ | -1.49 | -1.91 | -2.23 | -3.06 | $532\frac{5}{2}$ | 1.56 | 1.58 | 1.60 | 1.69 |
| | (0.243) | (0.311) | (0.364) | | | (0.401) | (0.421) | (0.436) | |
| $761\frac{3}{2}$ | -0.611 | -0.690 | -0.759 | -1.02 | $651\frac{1}{2}$ | 0.353 | -0.498 | -1.08 | -2.46 |
| | (0.296) | (0.338) | (0.372) | | | (-0.094) | (-0.217) | (-0.300) | |
| $880\frac{1}{2}$ | -1.18 | -1.64 | -2.02 | -3.06 | $651\frac{3}{2}$ | 1.77 | 1.85 | 1.92 | 2.15 |
| | (0.193) | (0.268) | (0.330) | | | (0.334) | (0.370) | (0.398) | |

column of Table I, the candidate orbitals to be assigned for this superdeformed band are [642]5/2, [651]3/2, [521]3/2, and [402]5/2 with $\Omega=K$ in the proton shell. Three of them except for [521]3/2 have positive parities.

### III. $g_K'$ VALUES

Now we calculated the renormalized $g_K$ factor, i.e., $g_K'$. We expand the state $|\sigma,\Omega\rangle$ by the spherical $j-j$ coupled wave function instead of (5),

$$|\sigma,\Omega\rangle=\sum U^{\sigma,\Omega}_{N,J,L,\Omega}|N,J,L,\Omega). \tag{7}$$

In (7) we drop the contribution from the unique-parity level, renormalize the wave function, and then estimate the $M1$ matrix element by this pseudospin wave function. We apply this method to the neutron shell of $^{192}$Hg and shows the calculated results in Fig. 4. We have not shown [505]11/2 in Fig. 4, as most of the components are from the unique-parity level, i.e., $h11/2$. Comparing Fig. 3 and Fig. 4, we see the renormalized $g_K'$ (Fig. 4) is quite different from the corresponding real $g_K$ (Fig. 3). If we use $g_K'$ values to explain the experimental data, there is no candidate level near Fermi surface around $\epsilon\sim0.5$ with $g_K=-0.65\pm0.14$ and $\Omega=2.8\pm0.8$ [5]. For example, $g_K'$ values for [512]5/2, [871]3/2, and [761]3/2 orbitals are now around $-0.41$ to $-0.47$, $g_K'$ for [631]3/2 is around $-0.24$, and that for [761]1/2 moves to $-1.28$ at $\epsilon\sim0.5$. Not only the absolute values of $g_K'$ but also its dependence on the deformation parameter is quite different from the original $g_K$ as is seen in [514]7/2, [640]1/2, [631]3/2, and [880]1/2 orbitals. Thus we cannot adjust by simply multiplying an effective factor to the renormalized $g_K'$ values in order to get the experimental

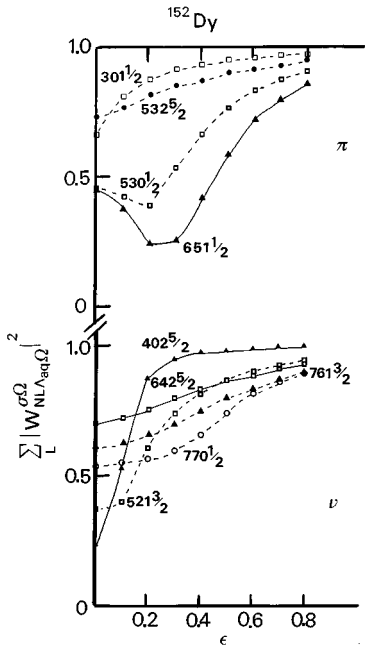


FIG. 5. The summed squared amplitudes of $|W^{\sigma,\Omega}_{N,L,\Lambda,\Omega}|^2$ with asymptotic value of $\Lambda_{aq}$ as a function of $\epsilon$ both for the neutron shell ($\nu$) and the proton shell ($\pi$) in $^{152}$Dy.

value. It is easily seen that the level which has the large component from the unique-parity level is much influenced by the renormalization procedure. In Fig. 4 [880]1/2, [871]3/2, [761]3/2, and [514]9/2 belong to the unique-parity family at the spherical limit. We see not only those levels which belong to the unique-parity family but also other levels which belong to the pseudospin family are much influenced by this renormalization. In the same way we calculated the renormalized $g_K'$ for the proton single-particle levels of $^{193}$Tl. Again $g_K'$ values are quite different from the original $g_K$ values. Around $\epsilon \sim 0.5$, $g_K'$ for [642]5/2 is 0.512, that for [651]3/2 is 1.25, for [521]3/2 is 1.36, and for [402]5/2 is 1.59. Here [642]5/2 and [651]3/2 belong to unique-parity family, while [521]3/2 and [402]5/2 to pseudospin family. Thus, we cannot neglect the influence from the unique-parity level on any state at superdeformation. As the authors of [7] calculated the $M1$ matrix element based on the real-spin picture and not on the pseudospin picture, their results are almost the same as ours and also support our conclusion.

Similarly we calculated the $^{152}$Dy case. We showed the values of calculated $g_K$ and $\langle \sigma,\Omega|s_z|\sigma,\Omega\rangle$ (inside the parentheses) as a function of $\epsilon$ in Table III. We can assume that the single-particle level of $^{152}$Dy is nearly the same as that of $^{153}$Dy and $^{153}$Ho. So Table III shows the prediction of the $g_K$ values for these nuclei. In the Dy case all the levels show a good convergence to the limit values except for [651]1/2 in the proton shell. This level gives only 44% of the limit value at $\epsilon = 0.7$, but again it is the case of negative expectation value of $s_z$, where the orbital term and the spin term in (2) cancels each other to interrupt the convergence.

In Fig. 5 we showed $\Sigma_L |W^{\sigma,\Omega}_{N,L,\Lambda,\Omega}|^2$ of $^{152}$Dy for one component of $\Lambda$ which coincides with the asymptotic value $\Lambda_{aq}$. The other component is easily obtained by subtracting this value from 1. All the levels, including [651]1/2 in the $\pi$ shell, show a good revival of $L-S$ coupling scheme in superdeformation.

## IV. CONCLUSION

In this work, we can assign several single-particle levels responsible for the observed $g_K$ values in $^{193}$Hg and $^{193}$Tl, and predict $g_K$ values for $^{153}$Dy and $^{153}$Ho in the superdeformed states. It is found that the convergence to the asymptotic limit $g_K$ value is interrupted by the subtraction between two components of $\Lambda = \Omega - 1/2$ and $\Lambda = \Omega + 1/2$ and the subtraction between the orbital part and the spin part for the level with asymptotic quantum number $\Omega = \Lambda - \frac{1}{2}$ in proton single-particle case. However, their wave functions show a quite good revival of the $L-S$ coupling scheme as is shown in Table II and Fig. 5. Comparing the renormalized $g_K'$ factor based on the pseudospin picture with the experimental data, we find that we cannot neglect the influence of the unique-parity level even for those levels belonging to the pseudospin family at superdeformation and the pseudospin picture is not suitable for the superdeformed band.

[1] K. Sugawara-Tanabe and A. Arima, Phys. Lett. B **317**,1 (1993); Nucl. Phys. **A557**, 157C (1993).
[2] K. Sugawara-Tanabe, A. Arima, and N. Yoshida, Phys. Rev. C **51**, 1809 (1995).
[3] A. Arima, M. Harvey, and K. Shimizu, Phys. Lett. **30B**, 517 (1969).
[4] K. T. Hecht and A. Adler, Nucl. Phys. **A137**, 129 (1969).
[5] M. J. Joyce *et al.*, Phys. Rev. Lett. **71**, 2176 (1993).
[6] J. F. Sharpey-Shafer, in *Proceedings of the IUPAP International Conference on Nuclear Physics*, Beijing, China, 1995 (World Scientific, Singapore, in press).
[7] P. B. Semmes, I. Ragnarsson, and S. Åberg, Phys. Lett. **345**, 185 (1995).
[8] T. Bengtsson, I. Ragnarsson, and S. Åberg, Comp. Nucl. Phys. **1**, 51 (1991).